

The applicability of an amidated polysaccharide hydrogel as a cartilage substitute: structural and rheological characterization

Gemma Leone,^a Maurizio Delfini,^b Maria Enrica Di Cocco,^b Anna Borioni^c
and Rolando Barbucci^{a,*}

^a*CRISMA and Department of Chemical and Biosystem Science and Technologies, University of Siena,
Via Aldo Moro 2, 53100 Siena, Italy*

^b*Department of Chemistry, 'La Sapienza' University, Piazzale Aldo Moro 5, 00185 Roma, Italy*

^c*Department of Research and Evaluation, ISS (Istituto Superiore di Sanità), Viale Regina Elena 299, 00161 Roma, Italy*

Received 27 July 2007; received in revised form 1 October 2007; accepted 9 October 2007

Available online 26 November 2007

Abstract—An amidic derivative of a carboxymethylcellulose-based hydrogel was obtained and characterized in terms of amidation degree. NMR studies and FT-IR imaging spectroscopy demonstrated that the reaction allowed a polymer to be obtained that was characterized by a regular distribution of amidic groups along the polysaccharide chains. Through this regularity, a homogenous three-dimensional scaffold was obtained, which maintained the thixotropic property of the linear polysaccharide.

© 2007 Elsevier Ltd. All rights reserved.

Keywords: Amidic carboxymethylcellulose; Hydrogel; NMR; FT-IR Imaging

1. Introduction

Articular cartilage is a thin layer of deformable, load-bearing material that lines the bony ends of all diarthrodial joints.¹ Macroscopic cartilage behavior depends on its complex microscopic structure. Its mechanical properties are determined by the composition of the tissue, mainly collagen and proteoglycans (chondroitin sulfate, hyaluronan, etc.), their assembly at the ultra-molecular level, and their interaction with interstitial fluids. The mixture of fluid and matrix provide the viscous-elastic and mechanical properties necessary for an efficient function of the cartilage tissue.^{2–5}

Recently, an amidic carboxymethylcellulose (CMCA) based hydrogel was utilized as a cartilage substitute in osteoarthritic rabbit.⁶ To elucidate hydrogel structure and water–polymer interaction, an analysis was performed by NMR and FT-IR imaging spectroscopy. Particular attention was focused on this aspect because the proteoglycan network, through its interaction with

both the collagen fibers and the interstitial water, plays a major role in the static and dynamic mechanical properties of the cartilage. The rheological and the swelling behavior of CMCA hydrogel were then studied.

2. Materials and methods

2.1. Materials

The sodium salt of CMC (viscosity 402 mPa s in 2% w/v aqueous solution at 25 °C and carboxymethylation degree of 0.9 ± 0.1 per monosaccharide unit $M_w = 200,000$) was supplied by Hercules Italia S.p.A (Italy). All the other reagents were purchased from Fluka Chemie AG (Switzerland).

2.2. Methods

2.2.1. Preparation of the amidic carboxymethylcellulose (CMCA) based hydrogel

2.2.1.1. Amidation of polysaccharide. The procedure used to obtain the amidic derivative of CMC was

* Corresponding author. Tel.: +39 577 234382; fax: +39 577 234383;
e-mail: barbucci@unisi.it

previously reported.⁷ Briefly, the CMC tetrabutylammonium salt (CMCTBA) was dissolved in *N,N'*-dimethylformamide (DMF) with mechanical stirring under a nitrogen flow. Once the polymer was completely dissolved, the temperature was lowered to 4 °C. The activating agent, 2-chloro-*N*-methylpyridinium iodide (CMP-I) was added in a stoichiometric amount compared to the percentage of carboxylic groups to be converted in amidic moieties. A 1:1 ratio of the amidating agent and alcoholic methylamine solution were added together with 2–3 drops of catalyst (ET₃N). The reaction was kept for 3 h and then the polysaccharide (CMCA) was precipitated by adding 95% ethanol and leaving the mixture overnight at 4 °C. The precipitate was separated by centrifugation (1500 rpm for 15 min), dissolved in water and dialyzed against 0.1 M NaCl for 48 h.

2.2.1.2. Cross-linking of amidic polysaccharide. The cross-linking reaction was carried out by dissolving the polysaccharide in the acidic form (CMCAH) in a mixture of DMSO–isopropanol (1:3) with mechanical stirring under a nitrogen flow. Then, 2-chloro-*N*-methylpyridinium iodide (CMP-I) was added to activate the remaining free carboxylic groups. The cross-linking agent, 1,3-diaminopropane (1,3-DAP), was added in a stoichiometric amount relative to the free carboxylic groups, which were to be cross-linked. Two to three drops of catalyst (ET₃N) were added and the reaction was kept for 3 h. The product hydrogel was purified by washing with doubly distilled water and ethanol. A ninhydrin assay was performed to check for the presence of unreacted NH₂ groups, resulting from the 1,3-DAP cross-linker.⁸

2.2.2. Physicochemical characterization of the polysaccharide (CMCA).

2.2.2.1. FTIR-ATR and imaging spectroscopy. ATR spectra of the samples, linear and cross-linked polysaccharides, in dry form were recorded on a Bio-Rad FTS6000 between 4000 and 750 cm⁻¹ following the classic procedure.⁹ The 1800–800 cm⁻¹ region, the most representative for the system, was studied. An MCT (mercury–cadmium–tellurium) detector was used and the apparatus was purged with nitrogen. As previously done, 64 scans at a resolution of 1.0 cm⁻¹ were averaged. The frequency scale was internally calibrated with a helium–neon reference laser to an accuracy of 0.01 cm⁻¹. Infrared images were measured with Thermo Nicolet Continuum Microscope (Madison, USA). The hydrogel sample was dried on to Petri dishes at 37 °C and placed on a BaF₂ crystal (13 × 2 mm). An area of 50 μm × 50 μm was scanned collecting 400 points.

2.2.2.2. Potentiometric titration. Potentiometric titrations were performed on the polysaccharide to evaluate the amidation degree. An aqueous solution of

the native polysaccharide (CMC) was subjected to Na⁺/H⁺ ion exchange using a weakly acidic exchanger resin (Amberlite CG-50) to obtain the polysaccharide in the acidic form (CMCH). Then, the CMCH polysaccharide was dissolved in a thermostatic glass cell at 25 °C at a constant ionic strength of 0.1 M NaCl with a known amount of 0.1 M HCl. The titration was performed with 0.1 M NaOH with back-titration using 0.1 M HCl. The default conditions for the experiment were as follows: a stabilization time of 600 s, a delay time of 5 min between each addition of titrant (25 μL). The titration was performed with a Mettler Toledo DL50 graphix titrator. Titration data were collected by LabX-mettler software and the titrated carboxylic groups were considered the reference amount corresponding to 100%. Then, the CMCA polysaccharide was titrated using the same procedure. The amidation degree of the polysaccharide was expressed as the percentage of the untitratable carboxylic groups with respect to the native CMC.¹⁰

2.2.2.3. High resolution NMR. High resolution NMR spectra were obtained on Bruker AVANCE 700 MHz and 400 MHz spectrometers operating, respectively, at 700.093 MHz for ¹H, 176 MHz for ¹³C and 400.062 MHz for ¹H, and at 100.577 MHz for ¹³C. The high resolution ¹H spectra were measured on polysaccharide and hydrogels swollen in deuterium oxide (ISOTEC Inc., 99.96% purity) at a controlled temperature of 310 ± 1 K, spectral width of 15 ppm, using a π/2 pulse, relaxation delay of 8 s, acquisition time of 3.5 s and a number of scans of 64. The high resolution ¹³C spectra, fully proton decoupled, were obtained with a 5 mm dual probe, a spectral width of 250 ppm, using a π/2 pulse, a relaxation delay of 9.5 s, an acquisition time of 0.5 s, and a number of scans of 10,000. Spectra were referenced to TSP (trimethylsilyl-*d*₄-propionate).

2.2.2.4. Low resolution NMR. Samples were prepared for low-resolution NMR measurements by swelling an exact amount of the cross-linked amidic carboxymethylcellulose with distilled water in a 10 mm NMR tube for 24 h at 310 ± 1 K. Experiments were performed on a Minispec PC120 pulsed NMR spectrometer with an operating frequency of 20 MHz for protons (magnetic field strength: 0.47 T). The NMR spectrometer was equipped with a pulsed gradient unit. Before the NMR measurements, a sample tube was placed into the NMR probe as long as needed to reach thermal equilibration (90 min). The measurements were performed at a temperature of 310 ± 1 K.

The longitudinal relaxation times (T₁) were determined by the standard inversion recovery (IR) sequence.¹¹ The relaxation recovery curves were fitted using NONLIN software (version 3.0). The transverse relaxation times (T₂) were measured using the

Carr–Purcell–Meiboom–Gill (CPMG) sequence.¹² The decay of the transverse magnetization was found to be constantly biexponential. The amplitudes and the spin–spin relaxation time of the two components were calculated by means of nonlinear least-squares data fitting with a home-written computer program based on the Marquardt algorithm.¹³

Water self-diffusion coefficient measurements were carried out using the standard pulsed field gradient spin echo (PFGSE) sequence.¹⁴ Keeping the gradient ampli-

tude G fixed, the amplitude of the NMR signal at a fixed echo time (AG) is given by:

$$AG = A_0 \exp(-kD)$$

where A_0 is the echo amplitude in absence of the pulsed gradients and k is given by $k = (gdG)^2 (D - d/3)$, where g is the proton magnetogyric ratio, and D is the time interval between the two gradient pulses of duration d . D values were determined by a monoexponential fitting of the echo amplitudes measured at different D values.

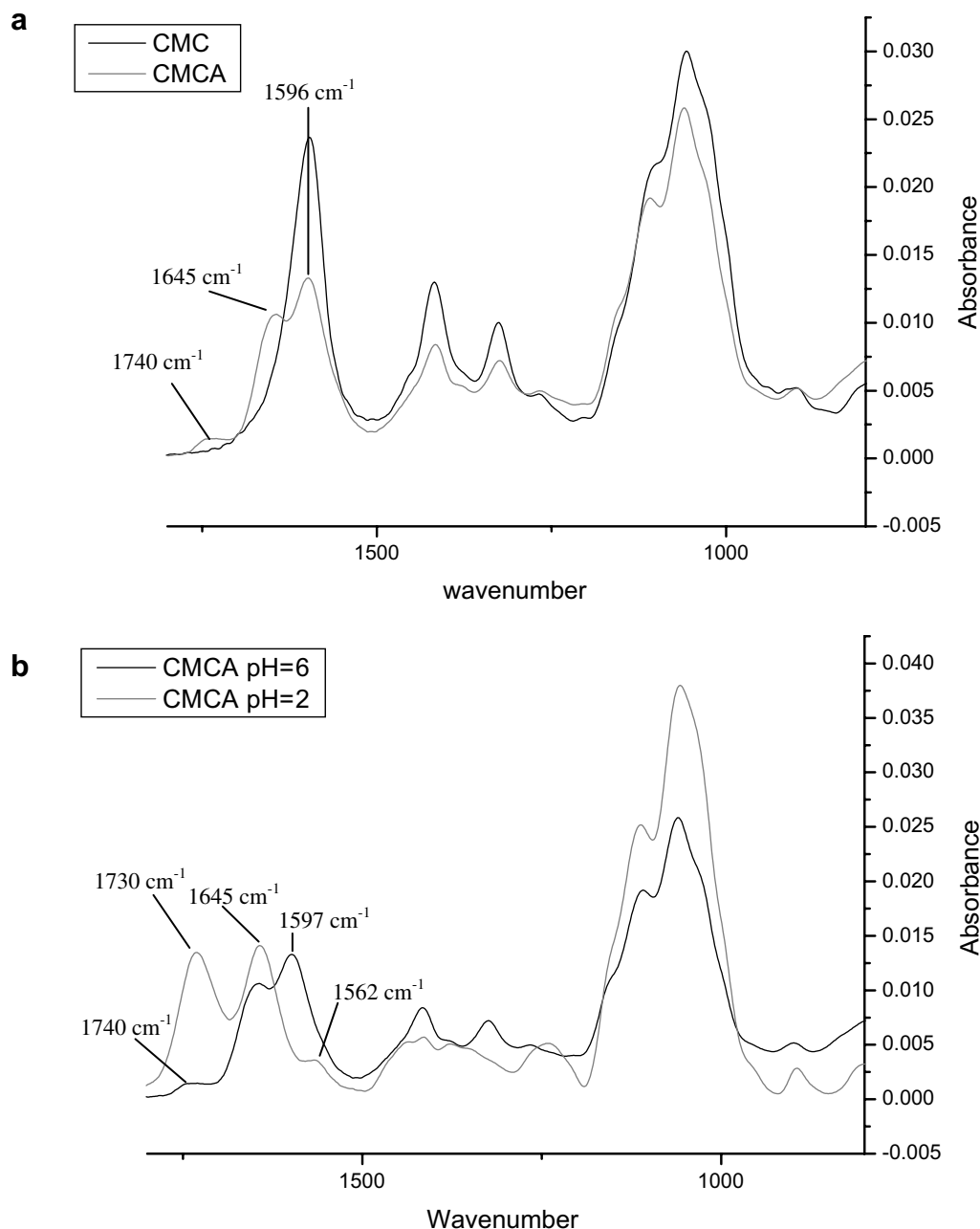


Figure 1. (a) IR spectrum of the most representative region (1800–800 cm⁻¹) of native CMC (black) and amidated CMCA (grey). The peak centered at 1645 cm⁻¹ is related to amidic C=O stretching; (b) IR spectrum of the most representative region (1800–800 cm⁻¹) of CMCA at pH 2 (black) and pH 6 (grey).

2.2.2.5. Water uptake measurements. Water up take (WU) was determined for the CMCA hydrogel with the following formula:

$$WU = [(W_s - W_d)/W_d] \times 100$$

where W_s and W_d are the weight of the swollen and dried hydrogel, respectively. In practice, a known amount of the dried sample was deposited on a propylene cell strainer with a nylon pore mesh of 100 μ m and immersed for several times at 25 °C in 50 mL of a buffer solution (pH 7.4: PBS). It was then placed on a piece of dry filter paper to remove the excess water. The filter containing the swollen hydrogel was weighed to calculate the water up take and the swelling kinetics.

2.2.2.6. Morphological analysis: scanning electron microscopy (SEM). Water swollen CMCA hydrogel (5 mg) was put into cryotubes and cooled by liquid nitrogen. After cooling, the hydrogel was lyophilized, mounted on SEM stubs and gold-sputtered by an automatic sputter coater (BAL-TEC SCD 050, Balzers, Germany). The sample was then observed using a XL20

SEM (Philips, The Netherlands) at 15 kV accelerating voltage.

2.2.2.7. Rheological analysis. The sample, in the swollen state (PBS pH7.4), was tested in a strain-controlled AR2000 Rheometer (TA-Instruments, Leatherhead, United Kingdom) in the parallel plate configuration. Smooth and rigid plates were used for testing. The plates were impermeable to fluid flow so as to reduce the free surface of the sample and minimize dehydration during testing. The small-amplitude oscillatory shear experiments were performed to measure the time-dependent response of the sample and hence, to determine its linear viscous elastic properties. A dynamic frequency sweep test was performed from 0.01 to 20 Hz at a maximum strain amplitude of 0.05, this range includes the knee physiological frequencies ranging from 0.5 Hz (walk) to 3 Hz (running).² In a dynamic experiment, the material is subjected to a sinusoidal shear strain and the mechanical response, expressed as shear stress of viscous-elastic materials is intermediate between an ideal, pure elastic solid (obeying Hooke's

Table 1. CMCA ^1H chemical shifts (ppm), assignments and relevant scalar correlations

Atom	Not substituted	Substitution on C2	Substitution on C3	Substitution on C6
H1	4.53	4.58	4.62	4.53
H2	3.55	3.40	3.55	3.55
H3	3.35	3.40	3.20	3.35
H4	3.67	3.67	3.76	3.67
H5	3.57	3.57	3.57	3.72
H6	3.97	3.97	3.97	3.79
H7	—	4.21–4.37	4.18–4.33	4.15–4.30

Table 2. CMCA ^{13}C chemical shifts (ppm), assignments and relevant scalar correlations

Atom	Not substituted	Substitution on C2	Substitution on C3	Substitution on C6
C1	101.62	102.64	103.66	101.62
C2	74.14	83.70	73.36	74.14
C3	74.11	80.05	82.46	74.11
C4	78.77	78.77	77.13	78.77
C5	75.31	75.31	75.31	76.30
C6	60.27	60.27	60.27	69.15
C7	—	71.67	71.67	70.69

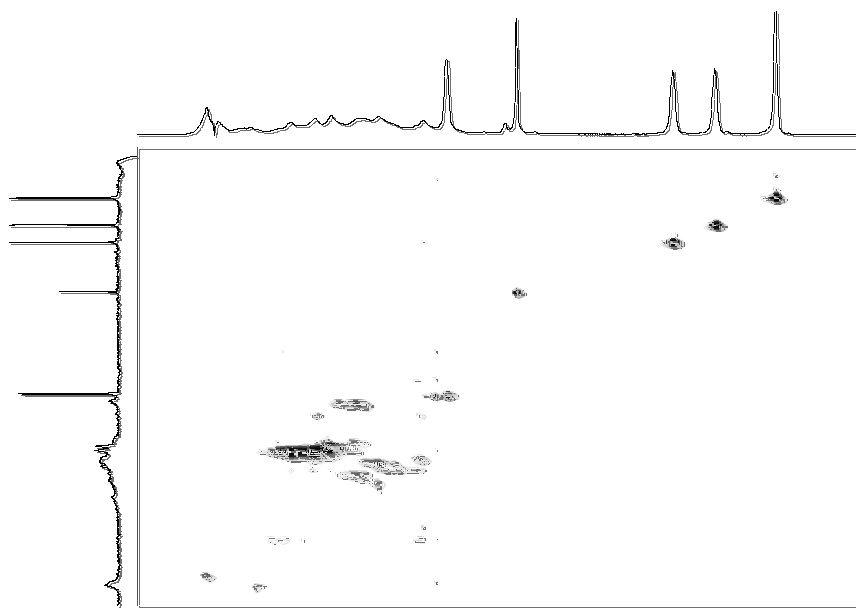


Figure 2. 2D hetero-correlated inverse experiments (HMQC and HMBC) of CMCA before cross-linking.

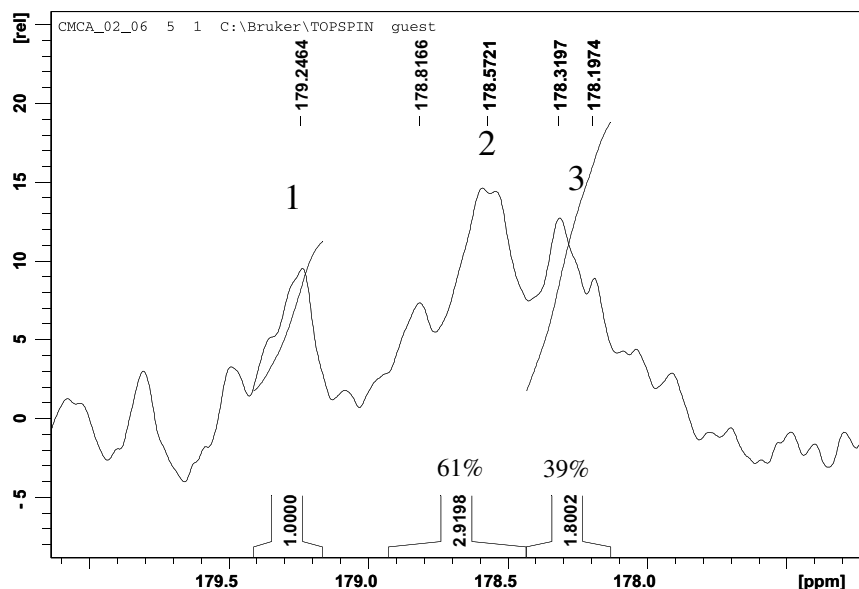


Figure 3. ^{13}C NMR spectrum of CMCA polysaccharide recorded at the controlled temperature of 310 ± 1 K.

law) and an ideal, pure viscous fluid (obeying Newton's law). The parameters which describe the viscous-elastic behavior are the shear storage modulus $G'(\omega)$ and the shear loss modulus $G''(\omega)$ and are dependent on the oscillation frequency (ω).

G' provides information about the elasticity or the energy stored in the material during deformation, whereas G'' describes the viscous character or the energy dissipated as heat. The ratio between the viscous and the elastic modulus is expressed by the loss tangent ($\tan\delta = G''/G'$) where δ is the phase angle. The loss tangent is a measure of the ratio of the energy lost against the energy stored in a cyclic deformation. A series of stress-relaxation experiments were performed to evaluate the shear stiffness at the equilibrium increasing the strain from 5% up to 20%.

3. Results and discussion

3.1. Structural characterization of amidic polysaccharide by infrared analysis, potentiometric titration and NMR spectroscopy

The amidation of the CMC polysaccharide was confirmed both qualitatively and quantitatively. The IR spectrum of the modified polysaccharide (CMCA) was compared with that of native polysaccharide (CMC). The CMCA IR spectrum showed a new shoulder centered at 1645 cm^{-1} which is related to the amidic C=O stretching.⁷ Furthermore, a new small peak centered at 1740 cm^{-1} , related to COOH groups, was present (Fig. 1a). In Figure 1b, the comparison between the IR spectra of CMCA polysaccharide at pH 2 and pH

6 is shown. At pH 2, the peak at 1597 cm^{-1} (COO^- asymmetric stretching) and the peak at 1740 cm^{-1} (COOH asymmetric stretching) disappeared, whereas just one peak centered at 1730 cm^{-1} (COOH , H-bonded) was present.

The amidation degree was also determined by potentiometric titration and NMR spectroscopy. Potentiometric titrations of the native CMC (used as reference) and the derivative CMCA were carried out and an amidation degree of 40% for CMCA polysaccharide was determined.

A complete structural NMR analysis of the polymer was carried out from which the amidation degree was also obtained. The structural aspects of CMCA were examined by ^1H and ^{13}C NMR spectroscopy. The ^1H NMR spectra showed broad and unresolved peaks due to the size of the macromolecules and to the presence of resonances arising from different substitution positions, so that univocal assignments were possible only on the basis of 2D ^1H NMR homonuclear COSY, TOCSY and 2D heterocorrelated inverse ^{13}C techniques as HMQC and HMBC. The assignments of the CMCA protons are reported in Table 1.

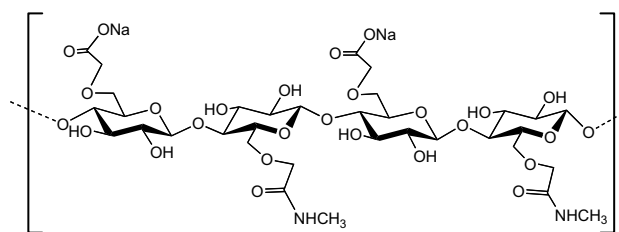


Figure 4. Schematic representation of the regular structure of CMCA polymer characterized by alternating carboxylic and amidic groups.

^{13}C NMR spectra were also recorded and the analysis confirmed the ^1H NMR data. Univocal assignments of

different carbon atoms in this case also were made possible only by 2D hetero-correlated inverse experiments

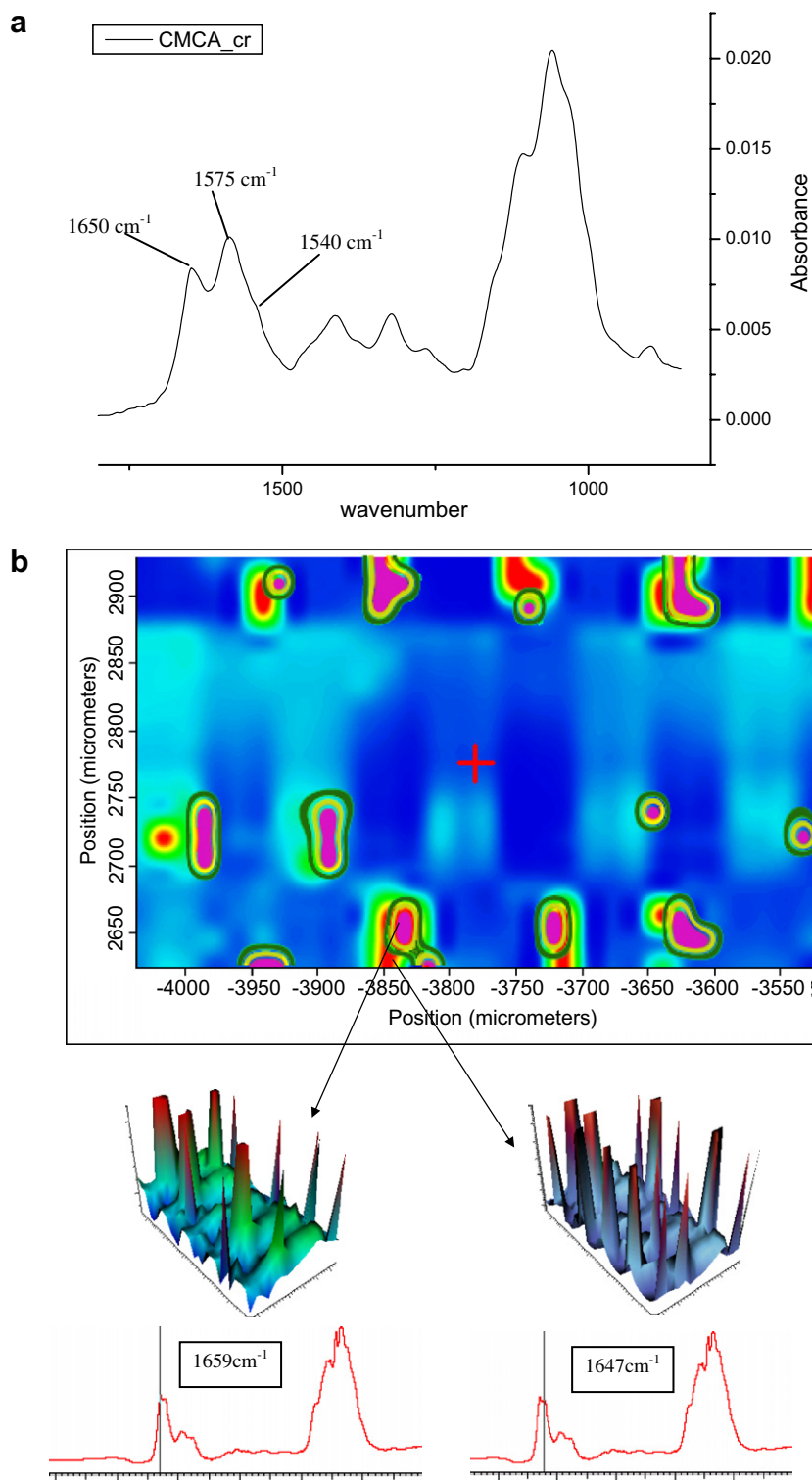


Figure 5. (a) The 1800–800 cm^{-1} region of IR spectrum of 100% CMCA based hydrogel. The cross-linking degree was confirmed by the absence of the peak related to COO^- asymmetric stretching (1597 cm^{-1}); (b) FT-IR image in which the red dots are related to CONHCH_3 amide groups (1647 cm^{-1}) and the pink dots to cross-linking amide groups (1659 cm^{-1}). The two different amide groups are very close to each other showing a regular alternation.

(HMQC and HMBC, Fig. 2). The ^{13}C chemical shifts, the assignments and the direct and long-range correlations are reported in Table 2.

The peak related to the carbonyl group was identified and assigned by comparing the NMR spectra of native CMC and CMCA. In the CMCA spectrum, a new complex signal was present at a higher field (178.3 ppm), which can be assigned to the amidic carbonyl group. ^{13}C experiments carried out without NOE allowed for the amidation degree to be calculated. This was calculated to be $\sim 39\%$, in good agreement with the potentiometric data (Fig. 3).

Furthermore, 2D NOESY experiments performed on differently diluted samples showed that the amidic and carboxylic groups were strictly alternating along the polysaccharide chains, thus confirming the regularity of the structure guaranteed by the chemical procedure performed. All these data allowed us to deduce the polysaccharide structure as reported in Figure 4.

3.2. Hydrogel structure

The amidic polysaccharide chains were cross-linked through a bridge derived from the formation of amidic bonds between the remaining carboxylic groups of the polysaccharides and the amine groups of the cross-linking agent, 1,3-diaminopropane. A 100% hydrogel (i.e., all the carboxylic groups not involved in the amidation

reaction were involved in the cross-linking reaction) was obtained by adding an excess of 2-chloro-*N*-methylpyridinium iodide to activate all the free carboxylic acid groups. The cross-linking reaction and the degree were confirmed by FT-IR spectroscopy (Fig. 5a). The IR spectrum showed an intense peak centered at 1575 cm^{-1} , which showed a very small shoulder centered at 1540 cm^{-1} . These two peaks can be related to the presence of two different kinds of amidic groups, the $-\text{CONHCH}_3$ and the cross-linking amidic groups. No evidence of free carboxylate groups was present (no absorbance at 1597 cm^{-1} , COO^- asymmetric stretching).

The two different amidic groups in the hydrogel were also mapped using the FT-IR imaging technique. As shown in Figure 5b, the red dots related to the $-\text{CONHCH}_3$ amidic groups of the polymer were positioned close to the pink dots, which were related to the new amidic groups formed on the carboxylic groups during the cross-linking reaction. This distribution confirmed the hypothesis of a regular distribution of $-\text{CONHCH}_3$ along the polymer chain.

3.3. NMR analysis of the hydrogel

The presence of cross-linking was first evidenced by the observation of a strong broadening of signals. In particular, C1 and C6 nuclei, not overlapped with other

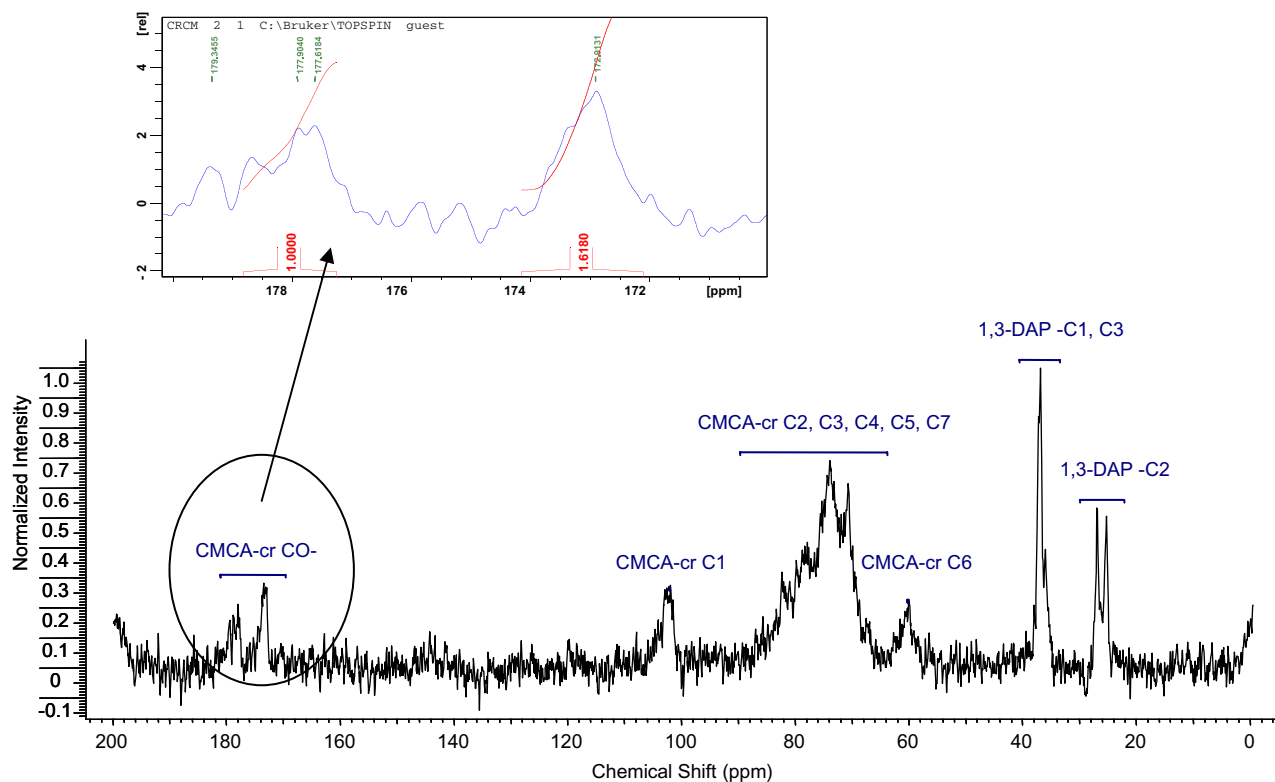


Figure 6. ^{13}C NMR spectrum of the CMCA hydrogel. The spectrum was recorded on a hydrogel swollen in deuterium oxide at the controlled temperature of $310 \pm 1\text{ K}$.

signals, showed a line width about 3–4 times greater than corresponding signals in the NMR spectrum of non cross-linked CMCA. The cross-linking reaction was confirmed also by the presence of new broad signals in the region between 25 and 35 ppm, which are related to the carbons of the 1,3-DAP cross-linking agent. Moreover, a very small percentage of impurity, free 1,3-DAP, was present as evidenced by the sharp signals as similar chemical shifts. The ^{13}C NMR spectrum of CMCA hydrogel showed no evidence of free carboxylic groups, whereas a new peak centered at about 175 ppm was found. This new peak was related to the new amidic $\text{C}=\text{O}$ groups deriving from the cross-linking reaction (Fig. 6).

3.4. Water–CMCA hydrogel interactions

Measurements of diffusional domains by low-resolution NMR spectroscopy performed on the hydrogels showed that a regular hydrogel structure could be obtained with reproducible meshes. The dimensions of the meshes depend on either the synthesis procedure or the amount of the activating agent added, but not on the polysaccharide. A similar result was previously obtained on four differently substituted hyaluronate (Hyal) hydrogels.¹⁵

Different values of water proton NMR relaxation times can be measured in heterogeneous systems such as hydrogels, due to the presence of different components and different compartments, that is, gel meshes or junction zones. Furthermore, water relaxation is affected by the polymer network structure as a result of water–macromolecule interactions. The relaxation curves, in general, and the decay magnetization curves,

in particular, show multi-exponential behavior in hydrogels. In fact, water can spread into the space between the meshes (bulk water) and within the meshes. Water can be seen as an integral part of the polymer structure or as trapped within interstitial spaces. Table 3 summarizes the values obtained for transverse relaxation times measured at 310 K.

Four different kinds of water were present. The component with the longer T_2 can be ascribed to water molecules remote from polymer network, called free water. The component with a lower T_2 can be ascribed to the water molecules whose motion is slightly affected by the presence of the polymer and, therefore, called bulk water. The reduced T_2 of bulk water can be simply explained as being due to the anisotropic motion that water molecules can undergo in a restricted region with possible further lowering due to proton exchange with polymer exchangeable protons. The fast relaxing component (meshes water) was attributed to the water molecules within the interstitial spaces of the polymer. Finally, the lowest T_2 can be ascribed to the water molecules strictly bound to the polymer chains. The same analysis has been previously performed on different hyaluronan based hydrogels with a 50% cross-linking degree.¹⁵ By comparing the T_2 values related to

Table 3. Transverse relaxation times and signal percentages of the two components of water in cross-linked amidic carboxymethylcellulose hydrogel at 310 K

Component	T_2 (ms)	%
Free water	2423 ± 30	22.5 ± 0.4
Bulk water	680 ± 14	39.1 ± 0.7
Meshes water	274.6 ± 3.6	36.2 ± 1.0
Bound water	12.25 ± 0.48	2.2 ± 0.1

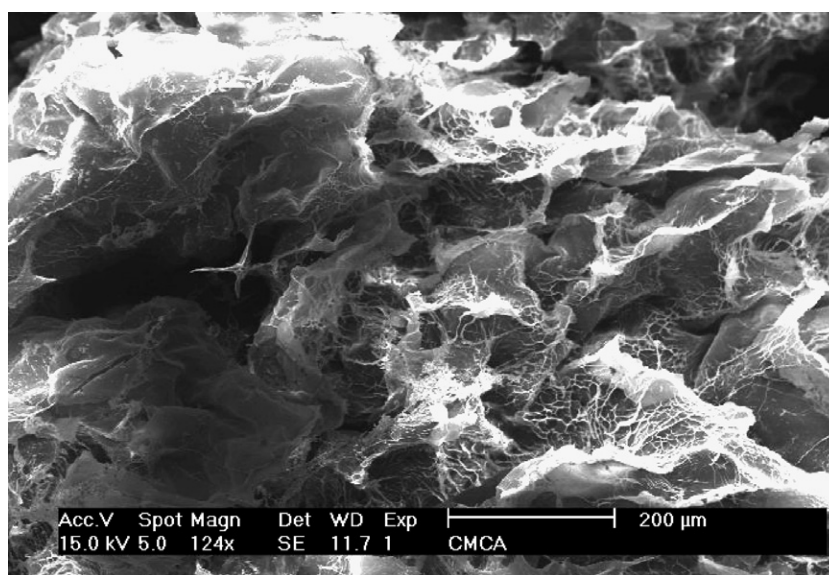


Figure 7. SEM micrograph of CMCA hydrogel recorded at 15.00 kV. The micrograph showed a homogeneous and opened structure with large fissures among the laminae.

the meshes, water paragonable values were found despite the higher cross-linking degree of the CMCA hydrogels, suggesting a high hydrophilicity of the CMCA polysaccharide. This hypothesis was confirmed also by the fact that for CMCA hydrogel a fourth slower water component was found, which can be related to the water strictly bound to the polymer.

3.5. Morphological analysis

Morphological analysis performed by SEM showed that the CMCA-based hydrogel possessed an open and homogeneous sponge-like structure, which was characterized by large fissures among the laminae (Fig. 7).

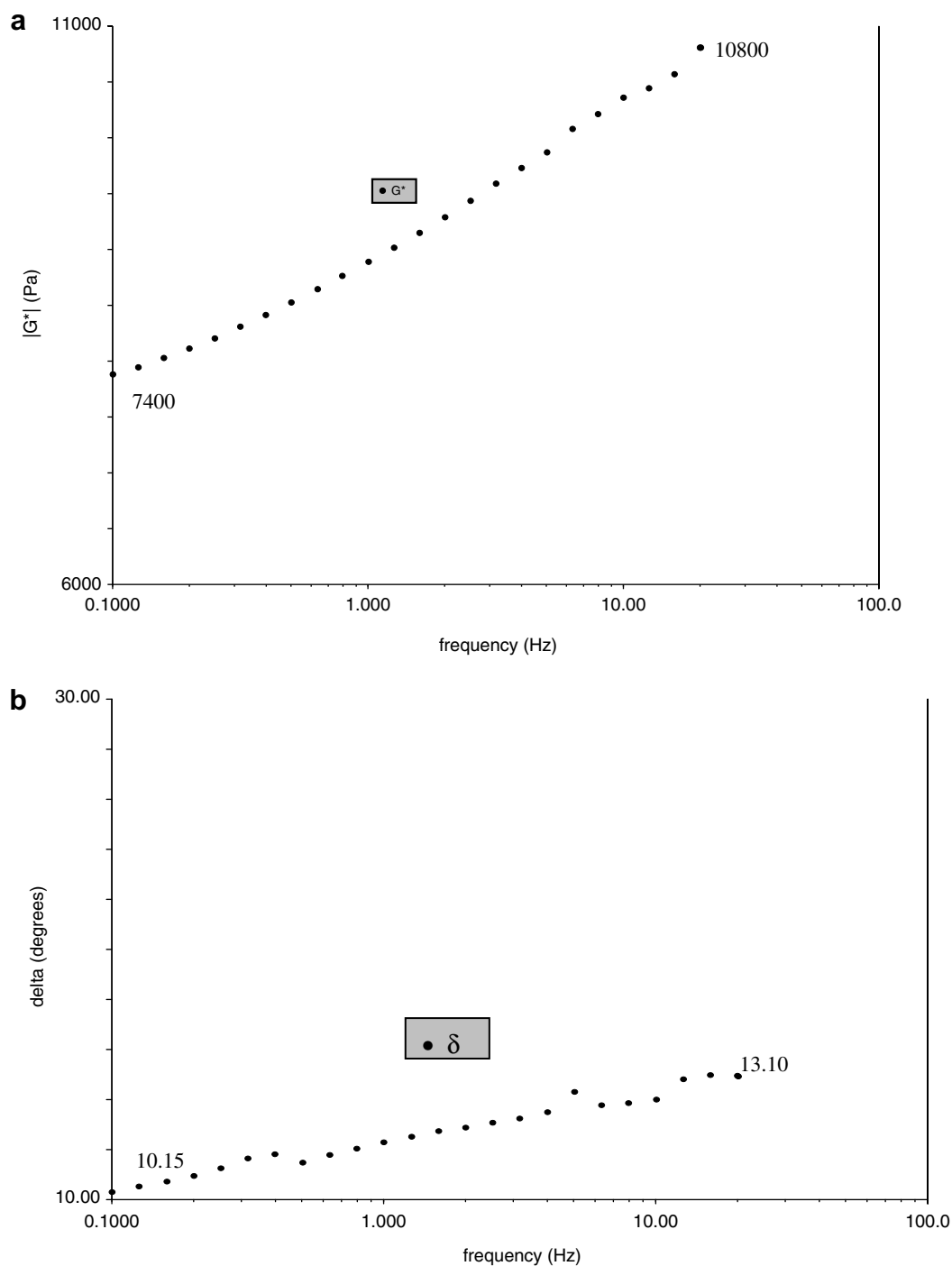


Figure 8. (a) Dynamic shear modulus ($|G^*|$, Pa) trend in the frequency range of (0.05–20 Hz) for CMCA hydrogel; (b) phase shift angle (δ , °) trend in the frequency range of (0.05–20 Hz) for CMCA hydrogel.

3.6. Rheological analysis

The equilibrium modulus (μ), a measure of the intrinsic matrix shear stiffness at equilibrium, and the dynamic modulus ($|G^*|$), a measure of combined elastic and viscous effects in dynamic shearing are important material properties for cartilage substitutes. The loss angle (δ) is a measure of the dissipation associated with viscous-elastic effects and can range from 0° for a perfectly elastic solid, to 90° for a perfectly viscous fluid. The frequency sweep test evidenced a ‘gel-like’ behavior for CMCA hydrogel, with the storage modulus (G') greater than the loss modulus (G'') within the frequency range analyzed. The CMCA hydrogel exhibited the typical behavior of a viscous-elastic solid under small deformation conditions. From both G' and G'' values, it was possible to obtain the trend of the complex shear modulus $|G^*|$ within the frequency range tested. It changed from 0.7 MPa (0.01 Hz) to 1.0 MPa (20 Hz) for CMCA (Fig. 8a). On the contrary, δ of the hydrogel did not change significantly over the range of the frequencies tested ($\sim 13^\circ$ for CMCA, Fig. 8b). The samples exhibited a predominantly elastic behavior in dynamic shearing, as evidenced by the value of $\delta < 45^\circ$, reflecting a more solid-like, rather than a fluid-like, behavior of the hydrogel under dynamic conditions.

The stress–relaxation test at a strain of 0.1 rad, performed to evaluate either the time dependent sensitivity to load or deformation of CMCA hydrogel, showed for the CMCA hydrogel a very rapid relaxation time within the first second after loading, to then slowly decay (Fig. 9).

The regularity of the polymer structure, characterized by alternating amidic and carboxylic groups, permitted a homogeneous network to be obtained and which was, as a consequence, able to respond to stress and dissipate quickly undergoing no fracture. This aspect,

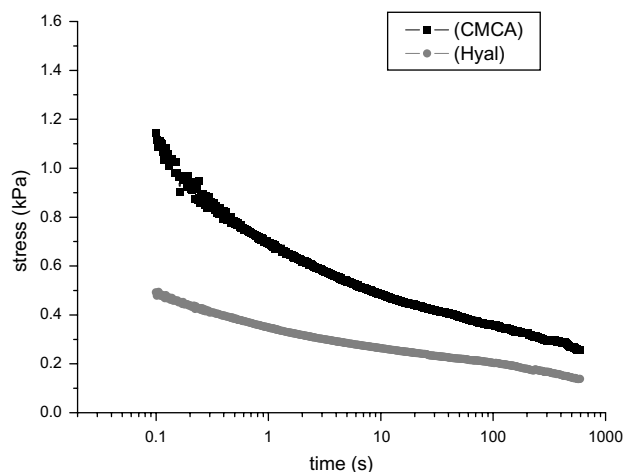


Figure 9. Behavior of CMCA hydrogel (black) subjected to a ramp stress-relaxation experiment with an imposed shear strain $\gamma_0 = 0.10$ rad.

together with the capability of the hydrogel to absorb a very large amount of water ($WU = 6000$ at pH 7.4), renders the hydrogel very similar to highly viscous solutions, allowing for the thixotropic behavior of the polysaccharide¹⁶ also in the hydrogel form.

In fact, the hydrogel obtained using the described procedure can be considered as formed by several macroparticles connected to each other by a diffused water network. When an appropriate stress is applied, the macroparticles slide on to the water layer, which connects them, and so under stress the system behaves as a fluid. Once the stress is removed, the hydrogel network formed again and the structure resumed its three-dimensional form. This property was observed in all the polysaccharide hydrogels obtained using our cross-linking procedure.¹⁷

4. Conclusions

An amidic derivative of carboxymethylcellulose-based hydrogel was obtained and characterized in terms of amidation degree. NMR studies and FT-IR imaging spectroscopy demonstrated that the reaction allowed a polymer to be obtained, which was characterized by a regular distribution of amidic groups along the polysaccharide chains. Through this regularity, a homogenous three-dimensional scaffold was obtained which maintained the thixotropic property as well as the linear polysaccharide.¹⁶ Furthermore, the rheological behavior of CMCA hydrogel, which may serve as potential filler for cartilage defects, showed that the CMCA hydrogel has the typical behavior of soft tissue in general, and of cartilage in particular. Because potential materials for artificial cartilage are required to be viscous-elastic, durable to repetitive stress, dissipative and low in friction,¹ this CMCA derivative performed in a similar way as cartilage.⁶ Actually, cartilage responds to shearing forces by both stretching and deformation of the solid matrix, so that in pure shear, the tissue is likely to deform with no change in volume, no pressure gradient and no fluid flow through the matrix.¹⁸ The rheological analysis showed that CMCA hydrogels showed a similar behavior, corroborated by the fact that by comparing the rheological performance of human cartilage and that of CMCA hydrogels, they appeared to be similar. The magnitude of the complex shear modulus [$|G^*| = (G'^2 + G''^2)^{1/2}$] of the cartilage increases monotonically from 0.2 MPa to 2.5 MPa, whereas within the same frequency range, the phase shift angle (δ) between solicitation and response varies between 9° and 22° [$\tan \delta = G''/G'$: energy dissipated during the shearing].¹⁹

A comparable behavior was found when comparing these values with those of CMCA with δ assuming a mean value of 13° for CMCA. Also, the complex modulus value was as comparable with that of cartilage.

Furthermore, the behavior of CMCA evidenced that the material was able to perform a cushioning function as against the knee activity and solicitations [walk (0.05 Hz), running (3 Hz)], without losing its mechanical characteristics as well as the human cartilage.^{1,5} The articular cartilage is a relatively high-compliant tissue having a shear modulus ranging from 0.2 to 0.4 MPa¹ and decaying very quickly. The CMCA hydrogel also showed a rapid relaxation within the first second.

Acknowledgement

The authors would like to thank the Fondazione Monte dei Paschi di Siena ('Traslazione clinica attuali conoscenze precliniche nell'ambito dell'ingegneria tessutale muscolo scheletrica per ricostruzioni biologiche da perdite di sostanza traumatiche o patologiche' project) for financial support.

References

1. Setton, L. A.; Elliott, D. M.; Mow, V. C. *Osteoarthr. Cartil.* **1999**, *7*, 2–14.
2. Mow, V. C.; Ratcliffe, A.; Poole, A. R. *Biomaterials* **1992**, *13*, 67–97.
3. Mow, V. C.; Ratcliffe, A.; Woo, S. L. Y. In *Biomechanics of Diarthrodial Joints*; Mow, V. C., Ratcliffe, A., Woo, S. L. Y., Eds.; Springer: New York, 1990.
4. Schimdt, M. B.; Mow, V. C.; Chun, L. E.; Eyre, D. R. *J. Orthop. Res.* **1990**, *8*, 353–363.
5. Netti, P. A.; Ambrosio, L. In *Integrated Biomaterials Science*; Barbucci, R., Ed.; Kluwer Academic: New York, 2002.
6. Leone, G.; Fini, M.; Torricelli, P.; Giardino, R.; Barbucci, R. *Osteoarthr. Cartil.*, submitted for publication.
7. Barbucci, R.; Leone, G.; Monici, M.; Pantalone, D.; Fini, M.; Giardino, R. *J. Mater. Chem.* **2005**, *22*, 2234–2241.
8. Virender, K. S.; Kent, S. B. H.; Tam, J. P.; Merrifield, R. B. *Anal. Biochem.* **1981**, *117*, 147–157.
9. Bellamy, L. J. *The Infrared Spectra of Complex Molecules*, 3rd ed.; Chapman and Hall: New York, 1980.
10. Barbucci, R.; Magnani, A.; Consumi, M. *Macromolecules* **2000**, *33*, 7475–7480.
11. Ernst, R. R.; Bosedhausen, G.; Wokaun, A. *Principles of Nuclear Magnetic Resonances in One and Two Dimensions*; Oxford Clarendon Press: New York, NY, 1991.
12. Meiboom, S.; Gill, D. *Rev. Sci. Instrum.* **1958**, *29*, 688–691.
13. Marquardt, D. W. *J. Soc. Ind. Appl. Mater.* **1963**, *11*, 431–441.
14. Stejskal, E. O.; Tanner, J. E. *J. Chem. Phys.* **1965**, *42*, 288–292.
15. Barbucci, R.; Leone, G.; Chiumiento, A.; Di Cocco, M. E.; D'Orazio, G.; Gianferri, G.; Delfini, M. *Carbohydr. Res.* **2006**, *341*, 1848–1858.
16. Zhang, L. M.; Kong, T. *Colloid Polym. Sci.* **2006**, *285*, 145–151.
17. Barbucci, R.; Leone, G.; Lamponi, S. *J. Biomed. Mater. Res.: Part B Appl. Biomater.* **2006**, *76B*, 33–40.
18. Zhu, W. B.; Koob, T. J.; Eyre, D. R. *J. Orthop. Res.* **1993**, *11*, 771–781.
19. Hayes, W. C.; Mockros, L. F. *J. Appl. Physiol.* **1971**, *31*, 562–568.